Coulomb effects in photoionization of H atoms irradiated by intense laser fields

AUTHOR(S):

Zhang, JT; Nakajima, T

PHYSICAL REVIEW A **75**, 043403 (2007)

Coulomb effects in photoionization of H atoms irradiated by intense laser fields

Jingtao Zhang* and Takashi Nakajima†
Institute of Advanced Energy, Kyoto University, Gokasho, Uji, Kyoto 611-0011, Japan
(Received 6 November 2006; published 12 April 2007)

We theoretically study the Coulomb effects on the photoionization processes of the H atom irradiated by the intense laser fields with circular and linear polarizations. For this purpose we represent the final continuum state by the Coulomb-Volkov state. Total ionization rates, photoelectron energy spectra, and angular distribution of photoelectrons are calculated and compared with those obtained using the Volkov state. We find that how much the Coulomb field influences the ionization dynamics depends on the momentum of photoelectrons, among which the photoelectron angular distributions in the linearly polarized laser field represent the most striking difference.

DOI: 10.1103/PhysRevA.75.043403 PACS number(s): 42.50.Hz, 32.80.Rm, 32.80.Fb

I. INTRODUCTION

In the theoretical study of photoionization of atoms in intense laser fields, an approach known as strong-field approximation (SFA) was frequently used [1]. Within the framework of SFA, it is assumed that a free electron having a well-defined momentum, described by the so-called Volkov state, interacts with the strong laser field, and the Coulomb interaction of the electron with the parent ion is completely neglected. In reality, however, due to the long-range nature of the Coulomb potential, an electron interacts with a laser field under the influence of the Coulomb potential. How much difference one would see by taking into account the Coulomb interaction is a question that requires a comprehensive study.

The effect of the Coulomb potential has many manifestations. In linearly polarized laser fields, the Coulomb potential is responsible for the appearance of a plateau in the photoelectron energy spectra (PES), which is caused by the rescattering of the ejected electron with a parent ion [2]. In elliptically polarized laser fields, the Coulomb field is responsible for the twofold symmetry in photoelectron angular distributions (PADs) [3]. Some effects come from the bound states supported by the Coulomb potential. For example, when atoms interact with short and intense laser pulses, the dynamic resonance with bound states takes place and results in the subpeaks in the above-threshold ionization spectra [4]. In a recent study, it has been found that the photoelectron ejection becomes asymmetric in space even in symmetrically distributed few-cycle laser fields [5,6]. Note that the use of the SFA by completely neglecting the Coulomb field cannot explain this asymmetry. That is, there are still many phenomena that cannot be fully explained by the SFA if one completely neglects the Coulomb field.

In order to study the Coulomb effects on the photoionization processes beyond the SFA, various kinds of corrections to the SFA have been developed. Those corrections can be classified into two categories: the first one is to make a correction in the SFA transition matrix, and the other is to make a correction in the Volkov state. In the first category, the twofold symmetry in elliptically polarized fields has been successfully explained in Ref. [7] by incorporating the Coulomb interaction as a first-order perturbation to the SFA transition matrix, which is based on the nonperturbative scattering theory of photoionization [8]. The theory developed in Ref. [8] has had notable success explaining the strong-field phenomena such as the splitting in the PAD and the jetlike structure in PADs reported in Refs. [9–12]. In addition, important progress has been recently reported in Ref. [13] to deal with the Coulomb-Volkov (CV) problem. Many other works fall into the second category, among which we note the work by two groups. In Refs. [14–17], the Coulomb interaction was taken into account only through the phase shift in the Volkov function, which decreases with increasing laser intensity so that the shift satisfies the expectation that the influence of the Coulomb field should become smaller with increasing laser intensity. In Refs. [18–27], the final state is represented by the CV state, i.e., in which the Coulomb function modulates in time due to the laser field in a similar manner as the Volkov plane-wave functions. In the CV states mentioned above, the influence of the Coulomb field is considered as a correction. For better accuracy, however, it is desired that the laser field and Coulomb field are treated on an equal footing [18]. This way, the CV state is reduced to the pure Coulomb function when the laser field is off, while it is reduced to the pure Volkov state when the Coulomb field is completely neglected [19]. Many authors used this kind of CV states for different purposes and we just cite some related works. An analytical formula for the transition matrix from the initial bound state to the final continuum state has been obtained in Ref. [20]. Based on this transition matrix, multiphoton ionization cross sections of H atoms in intense laser field have been studied in Refs. [25,26]. The most significant result using this CV state is the twofold symmetry found in PADs by elliptically polarized laser fields [24]. Recently, the validity of the CV state was examined by comparing the calculated PES with the numerical solution of the time-dependent Schrödinger equation (TDSE), and significant improvements in the CV approach have been made [28–34]. The improved CV approach allows one to perform the state-

*Permanent address: Shanghai Institute of Optical and Fine Mechanics, Chinese Academy of Sciences, P.O. Box 800-211, Shanghai 201800, China. Electronic address: jtzhang@siom.ac.cn
†Electronic address: t-nakajima@iae.kyoto-u.ac.jp

of-the-art calculations and to elicit the influence of the Coulomb interaction.

In this paper we employ the standard CV theory to study the Coulomb effects. The use of the standard CV approach has some advantages compared with numerically solving the TDSE: One of the advantages is that, by assuming the infinitely long laser pulse, one can obtain an analytical formula of the ionization rate in a closed form, which is very convenient as well as transparent to study the intensity-dependent photoionization processes. The formulas we derive also hold for the short pulse case, although strictly speaking we need to take into account the finite bandwidth effects arising from the short pulse duration, since the dominant ionization comes from the peak intensity rather than the bandwidth of shorter pulse duration. Thus, apart from the finite bandwidth effects for the short laser pulse, most of the features we find in this work could be recaptured even for the short pulse case. Another advantage is that the CV approach as well as SFA are beneficial over the TDSE method in terms of the computation time, in particular, when the intensity is very strong [28]. There are also some known limitations for the standard CV approach and the SFA: The first limitation is that they cannot take into account the depletion of the initial state [33,34] in the laser field, which is assumed to have an infinitely long pulse duration [20]. This, however, is not a big problem to investigate the influence of the Coulomb field, since, in real experimental situations, the main contribution to ionization comes around the peak of the pulse where the CV approach as well as SFA are valid. Thus, understanding the ionization dynamics in terms of the ionization rate rather than the ionization yield does not obscure the essence of strong field physics. The second limitation is a complete neglect of intermediate bound states in the CV approach and SFA [25,26], which implies that the CV treatment becomes a better one when other atomic intermediate states do not play a key role. This does not obscure the essence of strong field physics either, since in the intensity range where those two approaches are valid, ionization essentially comes from the initial (ground) state. Furthermore, it is known, as recently demonstrated in Refs. [32,35], that the intermediate bound states play an important role when the transition energy to the (first) excited state is close to the photon energy. For our specific case in which an intense laser field with long wavelength (800 nm) is irradiated to H atoms, excitation of the first excited state requires more than a few photons, which is very different from the situation assumed in Ref. [32]. This is another reason why intermediate bound states can be safely neglected in our case. Indeed, due to the reasons we have explained above, the CV approach as well as SFA are frequently employed to interpret the experimental data. In order for the CV approach to work even at lower intensities, one must improve the CV approach as recently reported by Gayet and his collaborators by taking into account the coupling between the initial and intermediate states [30–34].

Related to our work, the total ionization rates and the PADs for linear polarization have been studied using the CV state in Refs. [19,25], respectively, at the laser intensities below 10^{14} W/cm^2. For better understanding, a detailed study at intensities ranging from low to high intensities is desired. Furthermore, regardless of the fact that photoionization by circular polarization is known to differ very much from that by linear polarization, especially at low intensities, no report is found in the literature in this context using this CV state. As for the PES using this CV state, we do not find any report either. To summarize the past works using the CV states, we would like to emphasize that, although there are already some works as mentioned above, we find neither systematic nor comprehensive reports, which could lead to a clear, transparent, and unified physical picture in terms of the Coulomb effects upon photoionization.

In this paper we report the systematic as well as comprehensive study on the Coulomb effects upon photoionization of the H atom under the intense laser field with circular and linear polarizations. For that purpose we calculate the total photoionization rates, PES and PADs using the CV and Volkov states and compare them. We will show that, regardless of the intensities, the Coulomb potential strongly affects the low-energy photoelectrons, while its influence is weak for the high-energy photoelectrons. This feature is particularly clear in the PES, not to mention PADs. Some difference is also found in the total ionization rates, in particular, when the intensity is relatively low, and the difference becomes smaller and smaller with increasing laser intensity, as it should be. Although our CV calculations are not the best ones since we did not elaborate to improve our calculations for the CV by taking into account the pulse duration effects and excited states, the purpose of our paper is to understand the Coulomb effects by comparing the various physical quantities such as ionization rate, PES, and PAD.

This paper is arranged as follows: In order for this paper to be self-explanatory, we introduce the Volkov and CV states in Sec. II, and rederive the necessary formulas by the linearly polarized field in Sec. III. In Sec. IV, we present representative numerical results and discussions for the total ionization rates and PES for both linearly and circularly polarized fields, and PADs for linearly polarized fields. Finally, we conclude in Sec. V.

II. VOLKOV AND COULOMB-VOLKOV WAVE FUNCTIONS

The Volkov state is a wave function of a free electron moving in a laser field described by the vector potential $\mathbf{A}(t)$ [2] ($\hbar=1, c=1, e=|e|$),

$$\begin{aligned}\phi_V(\mathbf{p},t) &= (2\pi)^{-3/2}\exp\left[-i\int^t d\tau\frac{[\mathbf{p}+e\mathbf{A}(\tau)]^2}{2m_e}\right]\\ &\quad\times\exp\{i[\mathbf{p}+e\mathbf{A}(t)]\cdot\mathbf{r}\}\\ &= (2\pi)^{-3/2}\phi_{\mathbf{p}}(t)\exp[ieA(t)\boldsymbol{\epsilon}\cdot\mathbf{r}]\exp(i\mathbf{p}\cdot\mathbf{r}),\end{aligned}\quad (1)$$

where e and m_e are the charge and the mass of an electron, respectively; $\mathbf{r}$ denotes the position vector of an electron with respect to its parent cores and $\mathbf{p}$ is the corresponding conjugate momentum. If the laser field is a single mode with linear polarization, the vector potential $\mathbf{A}(t)$ can be written as $\mathbf{A}(t)=A_0\boldsymbol{\epsilon}\cos(\omega t)$, and correspondingly, the electric field is written as $\mathbf{E}(t)=\boldsymbol{\epsilon}E_0\sin(\omega t)$, where $\boldsymbol{\epsilon}$ is the real unit polarization vector, ω is the angular frequency of the laser field,

E_0 is the amplitude of the electric field, and $A_0=E_0/\omega$. The function $\phi_{\mathbf{p}}(t)$ is given by

$$\phi_{\mathbf{p}}(t)=\exp\{-i[(E_k+U_p)t+\lambda\sin(\omega t)+\rho\sin(2\omega t)]\}, \tag{2}$$

where E_k is the kinetic energy of the electron, U_p is the ponderomotive energy arising from the $\mathbf{A}(t)\cdot\mathbf{A}(t)$ term in Eq. (1), and $u_p=U_p/\omega$ is the ponderomotive parameter. The other two variables in $\phi_{\mathbf{p}}(t)$ are defined by

$$\lambda=\frac{e\mathbf{E}_0\cdot\mathbf{p}}{m_e\omega^2},$$

$$\rho=\frac{1}{2}u_p, \tag{3}$$

in which λ stems from the $\mathbf{p}\cdot\mathbf{A}(t)$ term in Eq. (1).

The CV state we employ consists of a Coulomb wave multiplied by a Volkov-type term, as first proposed by Jain and Tazor [18]. The Coulomb wave function is defined for the outgoing wave as [19,21]

$$u_{\mathbf{p}}^{(-)}(\mathbf{r},t)=N_{p1}F_1(-iv,1,-i(pr+\mathbf{p}\cdot\mathbf{r}))|\mathbf{p},t\rangle, \tag{4}$$

where $p=|\mathbf{p}|$ and v is a variable defined as $v=1/(a_0p)$ with a_0 being the Bohr radius. ${}_1F_1(a,b,z)$ is the confluent hypergeometric function of the first kind and $|\mathbf{p},t\rangle$ is the time-dependent plane wave with momentum $\mathbf{p}$,

$$|\mathbf{p},t\rangle=(2\pi)^{-3/2}\exp\left(-i\frac{p^2t}{2m_e}+i\mathbf{p}\cdot\mathbf{r}\right) \tag{5}$$

and

$$N_p=\exp(\pi v/2)\Gamma(1+iv), \tag{6}$$

with $\Gamma(x)$ being the Euler gamma function. Now the CV state can be obtained from Eq. (4) by replacing $\mathbf{p}$ by $\mathbf{p}+e\mathbf{A}(t)$ in its plane wave part as follows:

$$\begin{aligned}\Psi_{CV}(\mathbf{r},t)&=N_{p1}F_1(-iv,1,-i(pr+\mathbf{p}\cdot\mathbf{r}))|\mathbf{p}+e\mathbf{A}(t)\rangle\\&=\phi_{\mathbf{p}}(t)\exp[ieA(t)\boldsymbol{\epsilon}\cdot\mathbf{r}]u_{\mathbf{p}}^{(-)}(\mathbf{r}),\end{aligned} \tag{7}$$

where $u_{\mathbf{p}}^{(-)}(\mathbf{r})$ is given by

$$u_{\mathbf{p}}^{(-)}(\mathbf{r})=(2\pi)^{-3/2}N_{p1}F_1(-iv,1,-i(pr+\mathbf{p}\cdot\mathbf{r}))\exp(i\mathbf{p}\cdot\mathbf{r}). \tag{8}$$

The difference between the Volkov and CV states lies in $u_{\mathbf{p}}^{(-)}(\mathbf{r})$ given by Eq. (8), which is determined by the momentum and position of photoelectrons and is independent of the laser field. Clearly, when $v=0$, that is, in the limit of large photoelectron momentum $\mathbf{p}\to\infty$, the difference disappears and the CV state is reduced to the Volkov state.

In order to clearly show the difference between the Volkov and the CV states, we show their comparison in Figs. 1 and 2 in different conditions. Generally, the differences are more obvious for low-energy electrons. Figure 1 depicts the time-dependent parts of the Volkov and CV states as a function of r for $\mathbf{p}\cdot\mathbf{r}=pr$. We find that both real and imaginary parts oscillate with increasing r and the phase of the oscillation depends on the energy of electrons. The Volkov state oscillates regularly while that of the CV state does not, since the oscillation of the CV state also depends on the value of r. Furthermore, the amplitude of the CV changes rapidly with r at smaller distances. Figure 2 depicts the time-independent parts of the Volkov and CV states as a function of the angle between p and r for $|\mathbf{r}|=5a_0$. Here, the angle is defined as $\cos\theta=\mathbf{p}\cdot\mathbf{r}/(pr)$. Generally, the Volkov state is symmetric about $\pi/2$ but the CV state shows less symmetry. The real part of the Volkov state shown in the left column is symmetric about $\pi/2$, and the imaginary part shown in the right column is antisymmetric about $\pi/2$. This feature does not

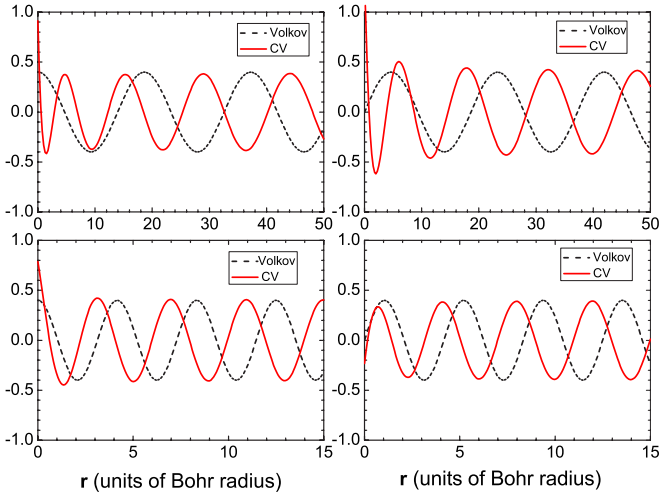

FIG. 1. (Color online) Time-independent parts of the CV (solid line), i.e., $u_p^{(-)}(\mathbf{r})$, and Volkov (dashed line) states, i.e., $\exp(i\mathbf{p}\cdot\mathbf{r})$, as a function of $\mathbf{r}$. The energy of electron is chosen to be 1.55 eV (top row) and 31.1 eV (bottom row). The left column is for the real part, and the right column for the imaginary part. We have set $\mathbf{p}\cdot\mathbf{r}=pr$.

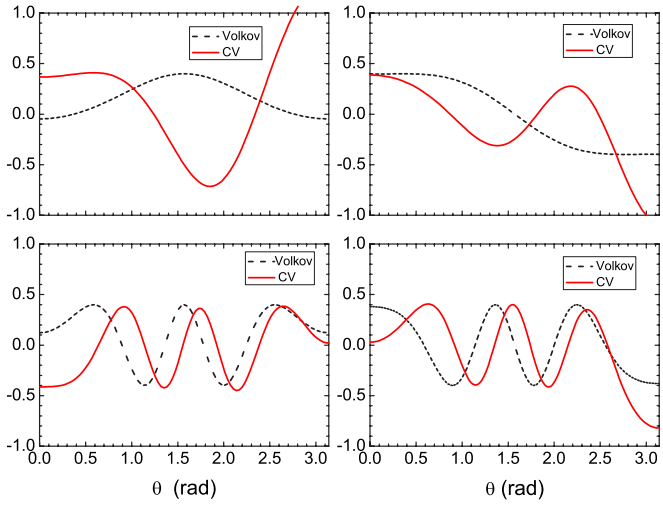

FIG. 2. (Color online) Time-independent parts of the CV (solid line), i.e., $u_p^{(-)}(\mathbf{r})$, and Volkov (dashed line) states, i.e., $\exp(i\mathbf{p}\cdot\mathbf{r})$, as a function of angle between the momentum $\mathbf{p}$ and the position $\mathbf{r}$ for $|\mathbf{r}|=5a_0$. The energy of electron is chosen to be 1.55 eV (top row) and 31.1 eV (bottom row). The left column is for the real part and the right column for the imaginary part.

vary with the momentum of electrons. For the CV state, the variation pattern is less symmetric and varies with the momentum of electrons. For low-energy electrons, as shown in the top row for electrons with energy 1.55 eV, both the real and imaginary parts do not show any symmetry. For high-energy electrons, as shown in the bottom row for electrons with energy 31.1 eV, oscillation appears and the CV state becomes more symmetric. Only for the electrons of very high energy (>200 eV), the CV state is almost symmetric and the difference between the Volkov and CV states is negligible.

III. IONIZATION-RATE FORMULA IN THE *E* GAUGE

In the *E* gauge (the electric field gauge), the ionization-rate formula using the CV state given by Eq. (7) was first obtained in Refs. [20,25]. In the *A* gauge (the radiation gauge), the ionization-rate formula was obtained using the Coulomb-corrected Volkov states in Refs. [14,15]. In this section, we present the detailed derivation of the ionization-rate formula in the *E* gauge using the Volkov as well as CV states.

We start with the transition matrix in scattering theory. The transition-matrix element can be written as [20]

$$T_{fi} = -i\int_{-\infty}^{\infty} dt\langle\Psi_f^{(-)}|e\mathbf{E}(t)\cdot\mathbf{r}|\Phi_i(\mathbf{r},t)\rangle, \tag{9}$$

where $\Psi_f^{(-)}$ is the final wave function of the outgoing electron in the presence of the laser field and the Coulomb potential, and is approximately given by the CV state in Eq. (7). $\Phi_i(\mathbf{r},t)$ is the initial wave function with binding energy I_0 and satisfies

$$H_0|\Phi_i(\mathbf{r},t)\rangle = I_0|\Phi_i(\mathbf{r},t)\rangle,$$

$$|\Phi_i(\mathbf{r},t)\rangle = |\Phi_i(\mathbf{r})\rangle e^{iI_0 t}. \tag{10}$$

Inserting Eq. (7) into Eq. (9), we obtain

$$T_{fi} = -ieE_0\int_{-\infty}^{\infty} dt e^{iI_0 t} S(\mathbf{p},\cos(\omega t))\sin(\omega t)\times\exp[i\lambda_k\sin(\omega t) + i\rho\sin(2\omega t) + i(E_k+U_p)t], \tag{11}$$

where $S(\mathbf{p},\cos(\omega t))$ is the space integral, which depends on the photoelectron momentum, the initial wave function, and time.

$$S(\mathbf{p},\cos(\omega t)) = \int d\mathbf{r}\exp[-ieA_0\cos(\omega t)\boldsymbol{\epsilon}\cdot\mathbf{r}]u_{\mathbf{p}}^{(-)*}(\mathbf{r})\times(\boldsymbol{\epsilon}\cdot\mathbf{r})\Phi_i(\mathbf{r}). \tag{12}$$

By making use of the following identities,

$$\exp[ix\sin(\omega t)] = \sum_{n=-\infty}^{\infty}\exp(in\omega t)J_n(x),$$

$$\exp[ix\cos(\omega t)] = \sum_{n=-\infty}^{\infty}(i)^j\exp(in\omega t)J_n(x), \tag{13}$$

Eq. (12) is rewritten as

$$S(\mathbf{p},\cos(\omega t)) = \sum_{n=-\infty}^{\infty}(i)^n\exp(in\omega t)\times\int d\mathbf{r}J_n(-eA_0\boldsymbol{\epsilon}\cdot\mathbf{r})u_{\mathbf{p}}^{(-)*}(\mathbf{r})(\boldsymbol{\epsilon}\cdot\mathbf{r})\Phi_i(\mathbf{r}). \tag{14}$$

Finally, the transition matrix defined by Eq. (9) is recast into the expression of

$$T_{fi} = ieE_0\sum_l (i)^l\delta(E_k+U_p+I_0-l\omega)\times\int_{-\pi}^{\pi} d\alpha\cos(\alpha)f_l(\alpha)S(\mathbf{p},\sin\alpha), \tag{15}$$

where $\alpha=\omega t$ and l stands for the number of photons absorbed before photoelectron ejection, and $f_l(\alpha)$ is given by

$$f_l(\alpha) = \exp(il\alpha - i\lambda\cos\alpha - i\rho\sin 2\alpha), \tag{16}$$

with λ and ρ being given by Eq. (3). Using the transition matrix, Eq. (15), the ionization rate after l-photon absorption is calculated with

$$\frac{dW_l}{d\Omega_p} = \int dp p_l^2|T_{fi}|^2\delta(E_k+I_0+U_p-l\omega), \tag{17}$$

in which $\mathbf{p}_l$ is the momentum of photoelectrons. Provided $dW_l/d\Omega_p$, the total ionization rate is computed by

$$\frac{dW}{d\Omega_p} = \sum_{l=l_0}\frac{dW_l}{d\Omega_p}, \tag{18}$$

where l_0 denotes the minimum number of photons necessary to overcome the binding potential, i.e., $l_0=\mathrm{int}[I_0/\omega+u_p]$. Expanding the energy delta function as [1]

$$\delta(E_k+I_0+U_p-l\omega) = (m_e/2\omega)^{1/2}(l-I_0/\omega-u_p)^{-1/2}\times\delta(p_l-(2m_e\omega)^{1/2}\times(l-I_0/\omega-u_p)^{1/2}), \tag{19}$$

and using the relation $a_0=4\pi/m_e e^2$, we find

$$\frac{dW_l}{d\Omega_p} = e^2 m_e E_0^2 p_l\left|\int_{-\pi}^{\pi} d\alpha\cos(\alpha)f_l(\alpha)S(\mathbf{p}_l,\sin\alpha)\right|^2. \tag{20}$$

Note that Eq. (20) holds for both the Volkov and CV states, since Eq. (12) is valid for any v, which includes $v=0$ representing Volkov states. The difference between the Volkov and the CV states lies in the S functions used in Eq. (20) [see Eq. (12)]. In the following sections, we explicitly derive the partial ionization rates for the Volkov and CV states, respectively.

A. Ionization-rate formula for Volkov states

Provided the energy of electrons, the SFA transition rate can be computed by

$$\frac{dW_l}{d\Omega_p} = \frac{4\pi E_0^2 p_l}{a_0}\left|\int_{-\pi}^{\pi} d\alpha \cos(\alpha) f_l(\alpha) S(\mathbf{p}_l, \sin\alpha)\right|^2, \quad (21)$$

where we have used the relation $a_0 = 4\pi/(e^2 m_e)$. For the H atom in the ground state $|100\rangle$, $S(\mathbf{p}_l, \sin\alpha)$ for Volkov states can be written as [16]

$$S(\mathbf{p}_l, \sin\alpha) = \frac{-i(2a_0)^{7/2}(\mathbf{p}_l + eA_0 \sin(\alpha)\boldsymbol{\epsilon})\cdot\boldsymbol{\epsilon}}{\pi[1 + a_0^2(\mathbf{p}_l + eA_0 \sin(\alpha)\boldsymbol{\epsilon})^2]^3}. \quad (22)$$

B. Ionization-rate formula for CV states

An analytical formula for $S(\mathbf{p}_l, \sin\alpha)$ for CV states was obtained in Ref. [20]. For hydrogen atom in the ground state $|100\rangle$, $S(\mathbf{p}, \sin\alpha)$ for linear polarization is given by

$$S(\mathbf{p}_l, \sin\alpha) = \frac{16\pi a_0^5 N_{p_l}^*}{(\pi a_0^3)^{1/2}} \frac{(1 - iv) M^{iv} \boldsymbol{\epsilon}\cdot[eA_0 \sin(\alpha)\boldsymbol{\epsilon} A + \mathbf{p}_l B]}{\{1 + a_0^2[eA_0 \sin(\alpha)\boldsymbol{\epsilon} + \mathbf{p}_l]^2\}^3}, \quad (23)$$

where

$$A = \left[-(2i + v) + (2v - i)M + \frac{(v - i)}{1 - iv}(1 + iv)M^2\right],$$

$$B = [2i + v - (v - i)M],$$

$$M = \frac{\{1 + [eA_0 \sin(\alpha)\boldsymbol{\epsilon} + \mathbf{p}]^2 a_0^2\}}{[(eA_0 \sin(\alpha))^2 a_0^2 - (pa_0 + i)^2]}. \quad (24)$$

For CV states, the transition rate given by Eq. (20) can be further simplified. Noting that

$$\Gamma(1 + iv)\Gamma(1 + iv)^* = -2\pi v \exp(-\pi v)[\exp(-2\pi v) - 1]^{-1}, \quad (25)$$

we find

$$\frac{dW_l}{d\Omega_p} = 2^8 a_0^3 E_0^2 [1 - \exp(-2\pi v)]^{-1} \times \left|\int_{-\pi}^{\pi} d\alpha \cos(\alpha) f_l(\alpha) S'(\mathbf{p}_l, \sin\alpha)\right|^2, \quad (26)$$

where

$$S'(\mathbf{p}_l, \sin\alpha) = \frac{(1 - iv) M^{iv} \boldsymbol{\epsilon}\cdot[eA_0 \sin(\alpha)\boldsymbol{\epsilon} A + \mathbf{p}_l B]}{\{1 + a_0^2[eA_0 \sin(\alpha)\boldsymbol{\epsilon} + \mathbf{p}_l]^2\}^3}, \quad (27)$$

and v should be calculated as $v = 1/(a_0 p_l)$.

IV. NUMERICAL RESULTS AND DISCUSSIONS

In this section, we calculate the total ionization rate and the PES by both linearly and circularly polarized laser fields, and PADs by linearly polarized laser fields. We also calculate the ionization rates for both Volkov and CV states, in accordance with the Reiss theory [1,14,15]. The laser wavelength of 800 nm is assumed throughout the calculations.

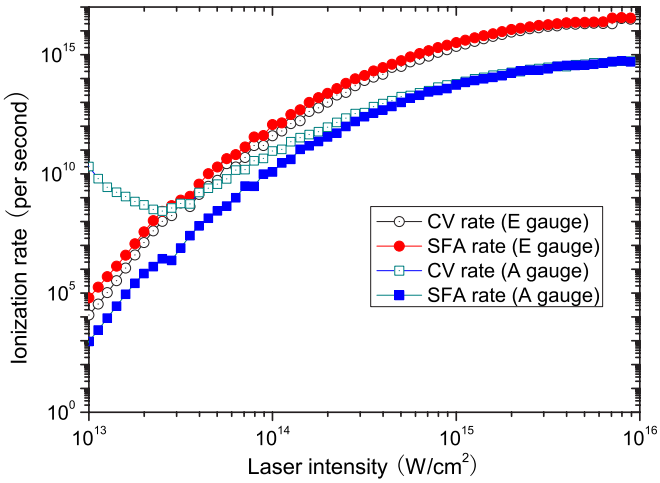

FIG. 3. (Color online) The variation of the total ionization rates as a function of laser intensity with linear polarization. The ionization rates in the E gauge are calculated according to the formulas presented in this paper, and the ionization rates in the A gauge are calculated according to the Reiss theory [1] (for the Volkov state) and the formula given by Bauer [15] (for the CV state). The wavelength of the incident laser is 800 nm.

A. Total ionization rate

Figure 3 depicts the variation of the total ionization rates for linear polarization as a function of laser intensity. Generally, the total ionization rates increase with laser intensity, and the increasing pattern also depends on the laser intensity. At the intensity below 10^{14} W/cm^2, the slope of the calculated ionization rates is large. As the laser intensity increases, the slope of the ionization rates becomes smaller and smaller. When the laser intensity is higher than 5×10^{15} W/cm^2 (a high-intensity regime), the ionization rates have little dependence on laser intensity, which is a feature of tunneling ionization. Note that the Keldysh parameter $\gamma = \sqrt{I_0/2U_p}$ at the high-intensity regime is less than 0.3. The difference between the CV and SFA ionization rates varies with the laser intensity. At the low-intensity regime, the CV ionization rate is smaller than the SFA ionization rate by about one order of magnitude. The difference becomes smaller as the laser intensity increases. At the high-intensity regime, the CV ionization rate is smaller than the SFA ionization rate by 1/3 or so, since ionization is mainly contributed by low-energy photoelectrons, which are strongly affected by the Coulomb attraction. We will give more explanation on this in the following sections.

Figure 3 also shows the total ionization rates by the A gauge. The CV and SFA ionization rates in the A gauge show a distinct difference at lower intensities, while the difference becomes smaller as the laser intensity increases and finally disappears at the high-intensity regime. This feature is seen for both linear and circular polarizations as we will show

below. In the treatment by Reiss *et al.* [14,15], the Coulomb potential causes a shift in the binding energy of the bound electron. The energy shift is large for lower laser intensities but tends to become zero as the laser intensity goes to infinity. Thus, it is natural to find a smaller difference at higher intensities. A difficulty in Reiss *et al.*'s treatment is that the energy shift becomes very large at lower intensities. For example, the energy shift for the H atom with a 800 nm laser is larger than the binding energy of the 1*s* electron if the laser intensity is lower than 2×10^{12} W/cm^2. Then the calculated ionization rate decreases with increasing laser intensity, which seems strange and unphysical. This implies that Reiss *et al.*'s Coulomb correction holds only for the high laser intensity ($>5\times10^{13}$ W/cm^2). When the ionization rates by the *E* gauge are compared with those by the *A* gauge, the results by the *E* gauge show a similar increasing pattern to the SFA ionization rate by the *A* gauge, but their values in the *E* gauge are always higher than those in the *A* gauge by about one order of magnitude. A possible explanation is as follows: The SFA ionization rate in Reiss *et al.*'s treatment is given by

$$\frac{dW_l}{d\Omega_p}=\frac{(2\omega^5)^{1/2}}{(2\pi)^2}|\Phi_i(\mathbf{p}_l)|^2(l-\epsilon_b-u_p)^{1/2}(l-u_p)^2J_l(\lambda,-\rho)^2. \tag{28}$$

Provided the photoelectron energy, there is only one transition channel with the probability amplitude described by the generalized Bessel function $J_l(\lambda,-\rho)$, while more channels are found in the present transition matrix [see Eq. (20)]. We notice that both CV and SFA ionization-rate formulas can be rewritten as

$$\begin{aligned}\frac{dW_l}{d\Omega_p}&\sim\left|\int_{-\pi}^{\pi}d\alpha\cos(\alpha)\exp(il\alpha-i\lambda\cos\alpha\right.\\&\quad\left.-i\rho\sin2\alpha)S(\mathbf{p}_l,\alpha)\right|^2\\&=\left|\sum_{n,m}(i)^nJ_n(-\lambda)J_m(\rho)\int_{-\pi}^{\pi}d\alpha\cos(\alpha)\exp[i(l+n\right.\\&\quad\left.-2m)\alpha]S(\mathbf{p}_l,\alpha)\right|^2.\end{aligned} \tag{29}$$

Numerical study shows that the integration over α becomes notable when $l+n-2m$ is an odd number, and there are double sums over n and m, respectively many transition channels are possible. Although multichannel transitions do not always mean a large transition rate, at least it makes a large transition rate possible. We should emphasize that the distinctive difference is not caused by the choice of the gauge. In Reiss *et al.*'s treatment, the Gorpprt-Mayer operator has been set to unity, thus only one transition channel survives [19]. In other treatments in the *A* gauge where multiple ionization channels are possible, the difference may not be so large [19]. A similar argument holds for circular polarization.

Figure 4 shows the calculated total ionization rates as a function of laser intensity for circular polarization for both *E* and *A* gauges. The ionization rates by the *E* gauge for circular polarization show similar dependence on the laser intensity as those for linear polarization, but the slope becomes more smooth. At the low-intensity regime, the ionization rate for circular polarization is far smaller than those for linear polarization, and the difference between the CV ionization rate and the SFA ionization rate is large. At the high-intensity regime, the CV and SFA ionization rates are almost identical to each other, and the ionization rates show little difference for linear and circular polarizations. A similar tendency has been found in Reiss *et al.*'s treatment [14,15], but the difference found in the present treatment is far smaller than that obtained by Reiss *et al.*'s treatment. For the circular polarization case, the difference in the total ionization rates between the *E* and *A* gauges is as large as 4 orders of magnitude in the high-intensity regime.

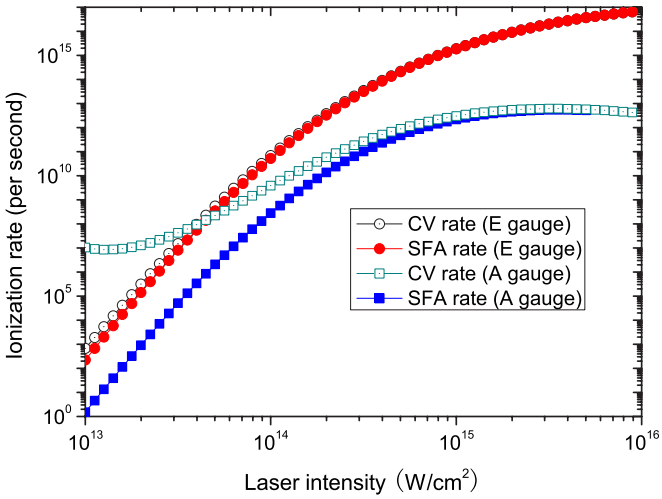

FIG. 4. (Color online) The same as that in Fig. 3, but for a circularly polarized laser field.

When we compare the calculated ionization rates for linear and circular polarizations, there are two points to be mentioned. The first one is that the ionization rate for linear polarization is much higher than that for circular polarization at the low-intensity regime, while the ionization rates are almost the same at the high-intensity regime. At the low-intensity regime, ionization is dominated by multiphoton ionization. Both experiments [36] and theories [37] revealed that the multiphoton ionization rate varies dramatically for different laser polarization. At the high-intensity regime, tunneling ionization or even the over-barrier ionization dominates the ionization process. As shown in the well-known Ammosov-Delone-Krainov theory [38], the ionization rate is independent of laser polarization and shows a slight variation on the laser intensity at the high-intensity regime. The second point is that the CV ionization rate in the *E* gauge is higher than the SFA ionization rate for circular polarization, but is lower than the SFA ionization rate for linear polarization. The comparison between the Volkov and CV states reveals the reason for this phenomenon. For linear polarization, the electrons in continuum states oscillate around the core in the polarization direction. As shown in Fig. 1, the CV state oscillates rapidly with r at a given direction. The rapid oscillation results in a smaller projection of the CV state onto

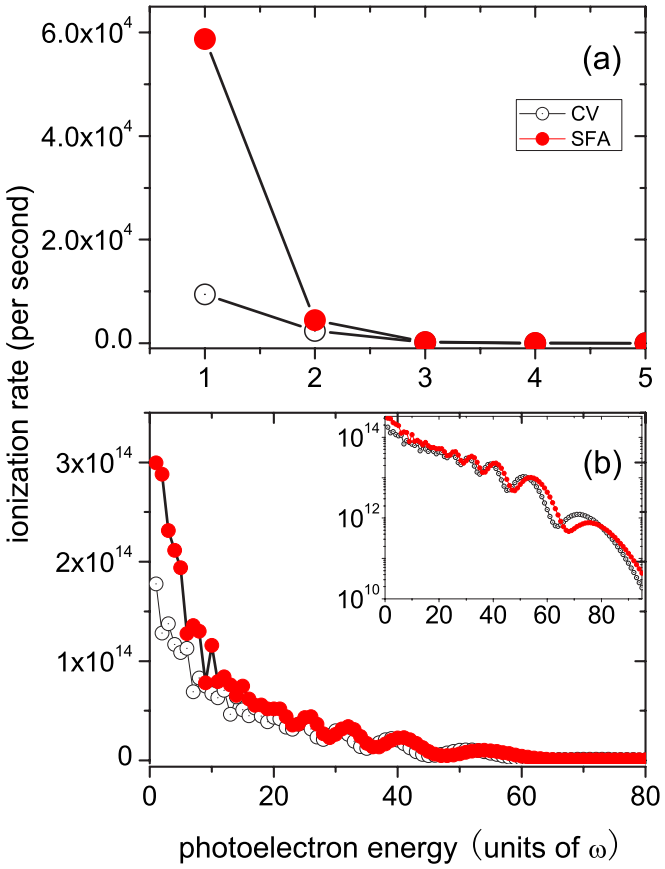

FIG. 5. (Color online) The photoelectrons energy spectra for linear polarization at the intensities of (a) 10^{13} W/cm^2 and (b) 10^{15} W/cm^2. The Inset in graph (b) is in a semilogarithmic scale.

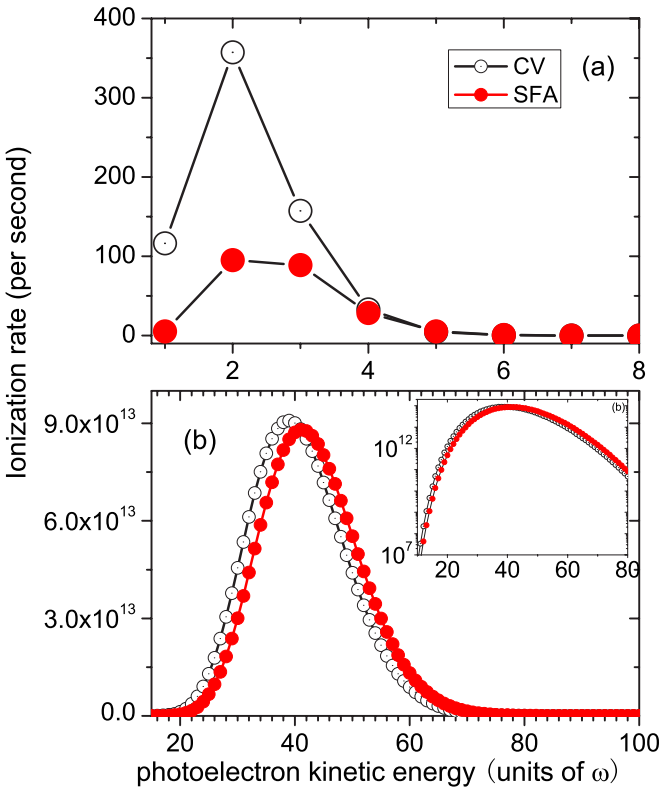

FIG. 6. (Color online) The photoelectrons energy spectra for circular polarization at the intensities of (a) 10^{13} W/cm^2 and (b) 10^{15} W/cm^2. The Inset in graph (b) is in a semilogarithmic scale.

the initial bound state. This is the reason why the CV ionization rate is smaller than the SFA ionization rate for linear polarization. For circular polarization, however, the electrons in continuum states move around the core in a circle vertical to the laser propagation. Thus, the rapid oscillation of the CV state with r plays little role. At a fixed value of $|\mathbf{r}|$ as shown in Fig. 2 for $|\mathbf{r}|=5a_0$, since the Volkov state is more symmetrically distributed over the angle than the CV state, the space integration for the Volkov state is generally smaller than that for the CV state. Thus, in general, the projection of the Volkov state onto the initial bound state has a smaller value for circular polarization. As a result, the CV ionization rate is higher than the SFA ionization rate for circular polarization.

The calculated results shown above approximately meet the expectation that the CV and SFA ionization rates are rather different at low intensities, while the difference becomes smaller and smaller with increasing laser intensity. Agreement of the CV and SFA ionization rates has been found to be better for circular polarization. Results on the PES to be presented in Sec. IV B shed some light on the physical understanding on the ionization dynamics by linearly and circularly polarized laser fields.

B. Photoelectron energy spectra

Figure 5 shows the calculated PES for the linearly polarized laser field. The low-energy electrons always have the highest yields, irrespective of the laser intensity. When the laser intensity is low, the yield of high-energy electrons decreases monotonically with the increasing energy, as shown in Fig. 5(a) for the laser intensity 10^{13} W/cm^2. In contrast, when the laser intensity is high, the yields of high-energy electrons do not always decrease monotonically with increasing energy, as shown in Fig. 5(b) for laser intensity 10^{15} W/cm^2. As a result, the PES show more structures. The PES for circular polarization is quite different from that for linear polarization, as shown in Fig. 6 for circular polarization. The lowest-energy electrons dominate the ionization signal only when the laser intensity is very low. As the laser intensity increases, the yield of low-energy electrons was suppressed and high-energy electrons dominate the ionization rate, as shown in Fig. 6(a). At the high-intensity regime, the yield of low-energy electrons are completely suppressed and the ionization rate is contributed mainly by the high-energy electrons, as shown in Fig. 6(b) and the PES exhibits a single broad peak at a high-energy region. This kind of spectra was first theoretically revealed by Corkum *et al.* and the suppression of low-energy electrons is attributed to a drift motion perpendicular to the electric field [39]. Generally, the calculated CV spectra show similar behavior to the SFA spectra, but shifts to the low-energy region due to the Coulomb attraction, as one can clearly see in Figs. 5(b) and 6(b).

A careful examination of the PES shown in Figs. 5 and 6 provides us with some insight on the difference of the CV

and SFA ionization rates we have presented in Figs. 3 and 4 for linear and circular polarizations. For that purpose, it is important to note that the high (small) momentum of photoelectrons implies that $v \to 0$ (∞), and the CV state is reduced to the Volkov state in the limit of $v \to 0$. For linear polarization, the ionization yield decreases with increasing energy of photoelectrons, although not always monotonically. The lowest energy photoelectrons $(l=l_0+1)$ always have the highest yield, no matter what the laser intensity is. This means that the total ionization rate is mainly contributed by those electrons with a larger value of v. Thus, even when the laser intensity is very high, the CV and SFA ionization rates still remain different, as we have seen in Fig. 3. However, the situation is very different for circular polarization. At lower intensities, the low-energy photoelectrons mainly contribute to the total ionization. Since the value of v is large, the influence of Coulomb potential is obvious, and hence the CV ionization rate shows a distinctive difference from the SFA ionization rate. At high intensities, the photoelectrons of relatively high energy have the highest yield thus dominate the total ionization. Since the value of v is smaller, the influence of Coulomb potential is smaller. Thus the difference between the CV and SFA ionization rates becomes smaller and smaller and finally negligible for circular polarization, as we have seen in Fig. 4.

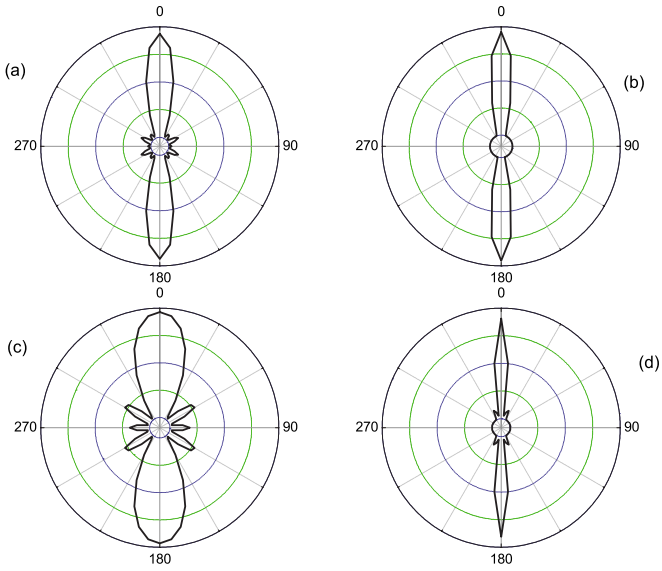

FIG. 7. (Color online) Polar plots of the PADs, obtained using the CV state, for the (a) first $(l=10)$ and (b) tenth $(l=19)$ peaks in the linearly polarized laser field at the intensity of 10^{13} W/cm^2. The plots in (c) and (d) are similar to (a) and (b), respectively, but calculated using the Volkov state.

C. Photoelectron angular distributions for linear polarization

The study of PADs provides even more information on the influence of the Coulomb potential. The PAD is calculated in the polarization plane (vertical to the wave vector) and the angle zero represents the direction of laser polarization. The calculated PADs for the linearly polarized field show rich structures: besides a main lobe around the direction of laser polarization, prominent electron "jets" appear at the waist of the main lobe. As the laser intensity and/or the kinetic energy of photoelectrons increases, more jets appear in the PADs. This result agrees with our earlier study on PADs [12]. Mathematically, the PADs depend on the laser intensity and the energy of photoelectrons, via the S function [see Eqs. (22) and (23)] and the f_l function [see Eq. (16)] in the transition matrix. Actually, the f_l function mainly determines the structure of PADs. The value of the transition matrix oscillatory increases with increasing value of λ, and the extrema form the jets in PADs. The larger the value of λ, the more the number of jets. The value of λ depends on the laser intensity and the momentum of photoelectrons.

Figures 7 and 8 show the polar plots of the PADs calculated at laser intensities 10^{13} W/cm^2 and 10^{14} W/cm^2, respectively. For comparison, the PADs using Volkov states are also shown. All the PADs have main lobes along the polarization vector and jets at the waist of PADs. The number of jets and the broadness of the main lobes indicate the difference between the CV and the SFA PADs. In particular, the CV PADs differ very much from the SFA PADs for low-energy (small l) electron, while they look quite similar to each other for high-energy (large l) electrons. Let us look at the PADs at 10^{14} W/cm^2 as an example. For low-energy photoelectrons, distinctive differences appear between the CV and SFA PADs, as shown in Figs. 8(a) and 8(d) for $l=13$ $(v=4.88)$. There are four jets in each side of the CV PAD shown in Fig. 8(a), while only two larger jets appear in each side of the SFA PAD shown in Fig. 8(d), and the main lobe in Fig. 8(d) split slightly. These differences originate from a strong influence of the Coulomb potential. For higher-energy photoelectrons, the difference becomes less evident, as shown in Figs. 8(c) and 8(f) for $l=32$ $(v=0.67)$. Although these two PADs have more jets, the jets are too small to be clearly seen, and the PADs are practically distributed along the laser polarization and look quite similar to each other.

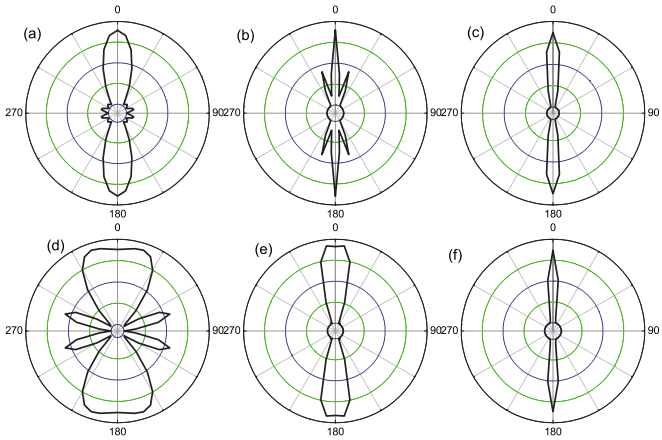

FIG. 8. (Color online) Polar plots of the PADs, obtained using the CV state, for the (a) first $(l=13)$, (b) tenth $(l=22)$, and (c) 20th $(l=32)$ peaks in the linearly polarized laser field at the intensity of 10^{14} W/cm^2. The plots in (d), (e), and (f) are similar to (a), (b), and (c), respectively, but calculated using the Volkov state.

V. CONCLUSIONS

In this paper we have theoretically studied the Coulomb effects on the photoionization processes of the H atom under the intense laser field with circular and linear polarizations. For that purpose, we have employed the CV and Volkov states to represent the final continuum, and compared the numerical results. We have found that how many Coulomb effects we can see depends critically on the energy of photoelectrons rather than on the intensities employed. In particular, the PADs by the linearly polarized laser field represent the most striking difference: For low-energy photoelectrons, a significant difference appears in the PADs using the CV and Volkov states. For higher-energy photoelectrons, on the other hand, the difference is not so evident, as expected. The Coulomb effects can also be clearly seen in the PES: the shift of the entire spectra to the low-energy side has been found when the CV states are employed instead of the Volkov states. For the linearly polarized laser field, the PES continuously extend from the low-energy to high-energy regions, and since the low-energy photoelectrons mainly contribute to the total (energy-integrated) ionization rate, the total ionization rates calculated by the CV and Volkov states still exhibit some difference even when the intensity is high. For the circularly polarized laser field, on the other hand, the PES exhibit a single broad peak in the high-energy region where the Coulomb field is negligible, resulting in no difference in terms of the total ionization rates at high intensities.

ACKNOWLEDGMENTS

J.Z. acknowledges the hospitality at Kyoto University during his stay. This work was supported by a Grant-in-aid for scientific research from the Ministry of Education and Science of Japan.

APPENDIX A: TRANSITION-RATE FORMULA FOR CIRCULAR POLARIZATION IN THE *E* GAUGE

For circular polarization, the SFA ionization rate after l-photon absorption is calculated as

$$\frac{dW_l}{d\Omega_p} = \frac{4\pi E_0^2 p_l}{a_0}\left|\int_{-\pi}^{\pi} d\alpha \cos(\alpha) f_l(\alpha) S(\mathbf{p}_l, \sin\alpha)\right|^2,$$

where $f_l(\alpha)$ is given by

$$f_l(\alpha) = \exp(il\alpha - i\lambda \cos\alpha/\sqrt{2}),$$

and $S(\mathbf{p}_l, \sin\alpha)$ is obtained from Eq. (22) by setting $\boldsymbol{\epsilon}\cdot\boldsymbol{\epsilon}=0$ and $A_0 \to A_0/\sqrt{2}$ as follows:

$$S(\mathbf{p}_l, \sin\alpha) = \frac{-i8a_0^{7/2}\boldsymbol{\epsilon}\cdot\mathbf{p}_l}{\pi\{1+a_0^2[p_l^2+\delta^2+2p_l\delta\sin(\alpha)]^2\}^3},$$

in which $\delta = eA_0/\sqrt{2}$, $\boldsymbol{\epsilon}\cdot\mathbf{p}_l = p_l\sin\theta$, and θ is the scattering angle varying from zero to π. The total ionization rate is obtained by sum over all possible l. The CV ionization rate after l-photon absorption is presented in Ref. [24]. We write it for clarity as follows:

$$\frac{dW_l}{d\Omega_p} = 2^8 a_0^3 E_0^2 [1-\exp(-2\pi v)]^{-1} \times \left|\int_{-\pi}^{\pi} d\alpha \cos(\alpha) f_l(\alpha) S'(\mathbf{p}_l, \sin\alpha)\right|^2,$$

where the $S'(\mathbf{p}_l, t)$ for CV state is given by

$$S'(\mathbf{p}_l, \sin\alpha) = \frac{(1-iv)M^{iv}\boldsymbol{\epsilon}\cdot\mathbf{p}_l}{\{1+a_0^2[\delta\sin\alpha\boldsymbol{\epsilon}+\mathbf{p}_l]^2\}^3\sqrt{2}}B$$

with the coefficient B as given by Eq. (24) in the text and

$$M = \frac{[1+(p^2+\delta^2+2\delta\boldsymbol{\epsilon}\cdot\mathbf{p}_l\sin\alpha)a_0^2]}{[(\delta a_0)^2-(p_l a_0+i)^2]}.$$

Other quantities are the same as that in the SFA ionization rate.

APPENDIX B: THE IONIZATION-RATE FORMULAS IN THE *A* GAUGE

The ionization rate in the A gauge was calculated according to Reiss *et al.*'s treatment. For linear polarization, the CV ionization rate after l-photon absorption is given by [15]

$$\frac{dW_l}{d\Omega_p} = \frac{(2\omega^5)^{1/2}}{(2\pi)^2}|\Phi_i(\mathbf{p}_l)|^2(l-\epsilon_b-u_p)^{1/2} \times \left[\sum_{m=-\infty}^{\infty}(l-u_p-2m)J_{l-2m}(\lambda,-\rho)J_m(\Delta_2)\right]^2,$$

where $\epsilon_b=(E_b-\Delta_1)/\omega$ with E_b the binding energy of the initial bound electron, Z is the nuclear charge,

$$\Delta_1 = \frac{Z}{\alpha_0}\frac{5}{4}, \quad \Delta_2 = \frac{Z}{\alpha_0}\frac{1}{8\omega},$$

and $\alpha_0=eE_0/(m_e\omega^2)$ is the radius of motion of a free electron in a circularly polarized laser field. For circular polarization, the CV ionization rate after l-photon absorption is given by Reiss and Krainov as [14]

$$\frac{dW_l}{d\Omega_p} = \frac{(2\omega^5)^{1/2}}{(2\pi)^2}|\Phi_i(\mathbf{p}_l)|^2(l-\epsilon_b-u_p)^{1/2}(l-u_p)^2 J_l(\lambda_c)^2,$$

where $\epsilon_b=(E_b-Z/\alpha_0)/\omega$. The corresponding SFA ionization-rate formula can be easily obtained by setting $\alpha_0\to\infty$.

[1] H. R. Reiss, Phys. Rev. A **22**, 1786 (1981).
[2] B. Walker, B. Sheehy, K. C. Kulander, and L. F. DiMauro, Phys. Rev. Lett. **77**, 5031 (1996); D. B. Milosevic, G. G. Paulus, and W. Becker, Opt. Express **11**, 1418 (2002).
[3] M. Bashkansky, P. H. Bucksbaum, and D. W. Schumacher, Phys. Rev. Lett. **60**, 2458 (1988).
[4] R. R. Freeman, P. H. Bucksbaum, H. Milchberg, S. Darack, D. Schumacher, and M. E. Geusic, Phys. Rev. Lett. **59**, 1092 (1987).
[5] S. Chelkowski and A. D. Bandrauk, Phys. Rev. A **71**, 053815 (2005).
[6] Xiaoming Zhang, Jingtao Zhang, Lihua Bai, Qihuang Gong, and Zhizhan Xu, Opt. Express **13**, 8708 (2005).
[7] Xingdong Mu, Phys. Rev. A **43**, 5149 (1991).
[8] D.-S. Guo, T. Aberg, and B. Crasemann, Phys. Rev. A **40**, 4997 (1989).
[9] D.-S. Guo and G. W. F. Drake, Phys. Rev. A **45**, 6622 (1992).
[10] P. H. Bucksbaum, D. W. Schumacher, and M. Bashkansky, Phys. Rev. Lett. **61**, 1182 (1988).
[11] M. J. Nandor, M. A. Walker, and L. D. Van Woerkom, J. Phys. B **31**, 4617 (1998).
[12] Jingtao Zhang, Wenqi Zhang, Zhizhan Xu, Xiaofeng Li, Panming Fu, D.-S. Guo, and R. R. Freeman, J. Phys. B **35**, 4809 (2002).
[13] D.-S. Guo, Y.-S. Wu, and L. Van Woerkom, Phys. Rev. A **73**, 023419 (2006); D.-S. Guo, R. R. Freeman, and Y.-S. Wu, J. Phys. A **33**, 7955 (2000).
[14] H. R. Reiss and V. P. Krainov, Phys. Rev. A **50**, R910 (1994); H. R. Reiss, *ibid.* **65**, 055405 (2002).
[15] J. Bauer, Phys. Rev. A **71**, 067401 (2005).
[16] K. Mishima, M. Hayashi, J. Yi, S. H. Lin, H. L. Selzle, and E. W. Schlag, Phys. Rev. A **66**, 053408 (2002).
[17] A. Becker, L. Plaja, P. Moreno, M. Nurhuda, and F. H. M. Faisal, Phys. Rev. A **64**, 023408 (2001).
[18] M. Jain and N. Tzoar, Phys. Rev. A **18**, 538 (1978).
[19] C. Leone, S. Bivona, R. Burlon, F. Morales, and G. Ferrante, Phys. Rev. A **40**, 1828 (1989).
[20] R. Burlon, C. Leone, S. Basile, F. Trombetta, and G. Ferrante, Phys. Rev. A **37**, 390 (1988).
[21] A. Cionga, V. Florescu, A. Maquet, and R. Taieb, Phys. Rev. A **47**, 1830 (1993).
[22] J. Z. Kaminski, A. Jaron, and F. Ehlotzky, Phys. Rev. A **53**, 1756 (1996).
[23] J. Z. Kaminski, Phys. Rev. A **37**, 622 (1988).
[24] S. Basile, F. Trombetta, and G. Ferrante, Phys. Rev. Lett. **61**, 2435 (1988).
[25] C. Leone, R. Burlon, F. Trometta, S. Basile, and G. Ferrante, Nuovo Cimento Soc. Ital. Fis., D **9**, 609 (1987).
[26] R. Burlon, C. Leone, F. Trometta, and G. Ferrante, Nuovo Cimento Soc. Ital. Fis., D **9**, 1033 (1987).
[27] S. Bivona, R. Burlon, C. Ferrante, and C. Leone, Opt. Express **14**, 3715 (2006).
[28] G. Duchateau, C. Illescas, B. Pons, E. Cormier, and R. Gayet, J. Phys. B **33**, L571 (2000).
[29] G. Duchateau, E. Cormier, H. Bachau, and R. Gayet, Phys. Rev. A **63**, 053411 (2001).
[30] G. Duchateau and R. Gayet, Phys. Rev. A **65**, 013405 (2001).
[31] G. Duchateau, E. Cormier, and R. Gayet, Phys. Rev. A **66**, 023412 (2002).
[32] V. D. Rodriguez, E. Cormier, and R. Gayet, Phys. Rev. A **69**, 053402 (2004).
[33] R. Gayet, J. Phys. B **38**, 3905 (2005).
[34] R. Guichard and R. Gayet, Phys. Rev. A **74**, 011402(R) (2006).
[35] Takashi Nakajima and Gabriela Buica, Phys. Rev. A **74**, 023411 (2006).
[36] M. Bashkansky, P. H. Bucksbaum, and D. W. Schumacher, Phys. Rev. Lett. **59**, 274 (1989); P. H. Bucksbaum, M. Bashkansky, R. R. Freeman, T. J. McIlrath, and L. F. DiMauro, Phys. Rev. Lett. **56**, 2590 (1986); G. G. Paulus, F. Zacher, H. Walther, A. Lohr, W. Becker, and M. Kleber, Phys. Rev. Lett. **80**, 484 (1998).
[37] S. Basile, G. Ferrante, and F. Trombetta, J. Phys. B **21**, L377 (1988).
[38] M. V. Ammosov, N. B. Delone, and V. P. Krainov, Zh. Eksp. Teor. Fiz. **91**, 2008 (1986) [Sov. Phys. JETP **64**, 1191 (1986)]; see also P. B. Corkum, Phys. Rev. Lett. **71**, 1994 (1993).
[39] P. B. Corkum, N. H. Burnett, and F. Brunel, Phys. Rev. Lett. **62**, 1259 (1989).